Improved anti-jamming scheme for direct-sequence spread-spectrum receivers

Weihua Dai✉, Chunjie Qiao, Yueke Wang and Chao Zhou

An anti-jamming scheme on the base band instead of the intermediate frequency (IF) is proposed to improve the anti-jamming capability of direct-sequence spread-spectrum (DSSS) receivers. For time–frequency domain technology, both the residual jamming energy and the unexpected loss of signal energy resulting from inaccurate jamming rejection would reduce the capability of signal acquisition. The scheme of detecting jamming by FFT and rejecting jamming by notch filters on the base band is exploited to improve the accuracy of jamming rejection. Monte Carlo simulation results show that the proposed scheme could enhance the anti-jamming capability of DSSS receivers.

Introduction: Direct-sequence spread-spectrum (DSSS) receivers have an inherent anti-jamming ability due to their spreading spectrum characteristics. Digital mobile phones and global positioning system (GPS) receivers may be the most familiar DSSS receivers. However, the function of a DSSS receiver would be weakened or even damaged, if the jamming energy is beyond the admitted level. As typical anti-jamming techniques, time–frequency domain (TFD) methods [1, 2] always detect jamming by spectrum analysis in the frequency domain (FD), and they reject jamming energy by filtering in the time domain (TD). Compared with other anti-jamming techniques, such as space domain [3], TD [4, 5] and FD [6], the TFD methods an detect jamming quickly; meanwhile the required hardware and computation are acceptable. However, jamming detection and rejection in DSSS receivers are always performed in the intermediate frequency (IF), which results in a high sampling rate, low frequency resolving and a limited anti-jamming ability for the TFD method.

In this Letter, the proposed scheme for TFD methods enhances the anti-jamming ability. Since it detects jamming on the base band, the frequency resolving can be improved to achieve a more accurate jamming detection, which is helpful to reject the jamming energy effectively by filtering. As a result, the anti-jamming ability is enhanced.

Proposed anti-jamming scheme: Without stepwise derivation from the analogue radio frequency signals received by the receiver antenna, the IF signal after the A/D convertor is modelled as

$$x(nT) = s(nT) + w(nT) + j(nT) \tag{1}$$

where T denotes the sampling period, $x(nT)$ denotes the digital IF signal, $s(nT)$ denotes the received DSSS signal and $w(nT)$ denotes the additive white Gaussian noise with zero mean and two-sided power spectral density $N_0/2$. $j(nT)$ denotes the continuous-wave interference (CWI) or jamming assumed to be multitone CWIs. In detail

$$s(nT) = \sqrt{2P_s}D(nT-\tau)C(nT-\tau)\cos\left[2\pi\left(f_d + f_{IF}\right)nT + \theta\right] \tag{2}$$

$$j(nT) = \sum_{i=1}^{K}\sqrt{2P_{j,i}}\cos\left(2\pi f_{j,i}nT + \theta_{j,i}\right) \tag{3}$$

where P_s is the power of the signal; $C(nT-\tau)$ is the spread spectrum code; $D(nT-\tau)$ is the transmitted symbol data, which is assumed to be 1 for simplicity; τ is the delay introduced by the transmission channel; f_d and θ are the corresponding Doppler frequency and the phase offset, respectively; and f_{IF} is the IF. K is the number of CWIs; $P_{j,i}$, $f_{j,i}$ and $\theta_{j,i}$ are the power, frequency and phase delays of the ith jamming signal, respectively. The jamming-to-signal ratio (JSR) for the ith jamming signal is defined as

$$\mathrm{JSR}_i = 10\log_{10}\left\{\frac{P_{j,i}}{P_s}\right\} \tag{4}$$

Real IF signals are always truncated to detect the jamming frequency in the conditional TFD method, and they would be filtered before converting to a base band signal if the jamming energy exceeds the threshold value. Differently, the real IF signals are downconverted to complex base band signals firstly in the proposed scheme, and complex base band signals are truncated for jamming detection, and they would be filtered by notch filters if the jamming frequency is detected. A conditional reference scheme and the proposed scheme are shown in Fig. 1.

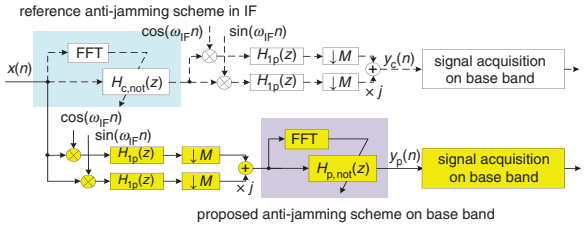

Fig. 1 *Comparison of reference scheme and proposed scheme*

Fig. 1 shows that the IF signals are demodulated by the in-phase local carrier and the quadrature-phase local carrier with angular frequency $\omega_{IF} = 2\pi T f_{IF}$ during the downconverting process, and the high frequency components are filtered by lowpass filters with a linear phase. Two channel filtering outputs are both downsampled with M times, and subsequently united as complex signals, which are inputted to the signal acquisition module. The notch filter of the reference scheme is a cascade of second-order IIR filters, the transfer function of which is

$$H_{c,not}(z) = \prod_{i=1}^{K}\frac{1 - 2\cos(\hat{\omega}_i)z^{-1} + z^{-2}}{1 - 2\alpha\cos(\hat{\omega}_i)z^{-1} + \alpha^2 z^{-2}} \tag{5}$$

The notch filter of proposed scheme is a cascade of first-order IIR filters

$$H_{p,not}(z) = \prod_{i=1}^{K}\frac{1 - e^{j\hat{\omega}_i}z^{-1}}{1 - \alpha e^{j\hat{\omega}_i}z^{-1}} \tag{6}$$

where α is an adjustable parameter ranging from 0 to 1; $\hat{\omega}_i$ is the detected normalised jamming frequency in rad/seconds, namely, there is $\hat{\omega}_i = 2\pi T\hat{f}_{c,i}$ in the reference scheme while there is $\hat{\omega}_i = 2\pi MT\hat{f}_{p,i}$ in the proposed scheme. $\hat{f}_{c,i}$ and $\hat{f}_{p,i}$ denote the detected jamming frequency in hertzing in the reference scheme and the proposed scheme, respectively. Assume that the detection error is ignored, there exists $\hat{f}_{p,i} = \hat{f}_{c,i} - f_{IF}$. However, the detection error always exists, and it would mainly be determined by the frequency resolving if the jamming power is strong. Obviously, the frequency resolving in the proposed scheme could be M times higher than the one in the reference scheme for the same length FFT. It could lead to more accurate jamming detection in the proposed scheme than in the reference scheme.

Moreover, it is more feasible to configure the parameter α for achieving an appropriate notch width in the proposed scheme than in the reference scheme. The amplitude responses of the first-order notch filter or the second-order notch filter with the notch frequency 0.49π rad/s for some α are shown between 0 and π rad/s in Fig. 2. The notch width is in proportion to the value $(1-\alpha)$. Actually, the notch width in hertz is also in proportion to the sampling rate f, which is described as $\mathrm{Band}_{not} \propto (1-\alpha)f$. Therefore, the larger α and smaller sampling rate are desired to keep the signal energy as high as possible. Thus, compared with the proposed scheme, the reference scheme should use a larger α for achieving the same notch width, which may be not well supported by its low frequency resolving and jamming detection accuracy.

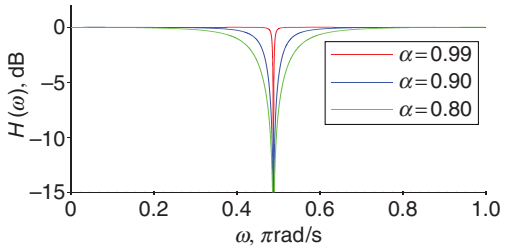

Fig. 2 *Amplitude response of notch filter for different* α

Experiment and simulation results: Simulation and experimental results were performed to verify the feasibility and the performance of the proposed scheme. All the experiments were implemented by M-files in MATLAB R2009a. The GPS C/A code with chip rate $R_c = 1.023$ MHz is used as the spread spectrum code, and only its energy in the main lobe are reserved by roll-off. Some fixed parameters

are as follows: $f_{IF} = 4.096$ MHz; $F = 8f_{IF}$; $f_{j,1} = 3.342$ MHz; $f_{j,2} = 4.342$ MHz. An M-order CIC filter is used as the lowpass filter.

Some experiments were performed to illustrate the anti-jamming effectivity of the reference scheme and the proposed scheme. Other parameters are as follows: $P_s = 1$; $N_0 = 0$; $P_{j,i} = 0.1$; $\tau = 0$ s; $f_d = 0$ kHz; and θ, $\theta_{j,i} = 0$ rad/s. Fig. 3 illustrates the results of numerical simulation for $\alpha = 0.99$ and $M = 4$. Fig. 3*a* shows the referenced power spectral of the clean base band signal; Fig. 3*b* shows the power spectral of base band signal polluted by jamming; Fig. 3*c* shows the power spectral of the filtered base band signal in the reference scheme; Fig. 3*d* shows the power spectral of the filtered base band signal in the proposed scheme. It is found that the jamming energy is rejected effectively both in Figs. 3*c* and *d*. However, the reserved energy in Fig. 3*c* is less than that in Fig. 3*d*, which demonstrates the improved performance of the proposed scheme. Furthermore, the power ratio of $y_c(n)$ to $y_0(n)$ (normal font) and the power ratio of $y_p(n)$ to $y_0(n)$ (bold font) for some α and M are shown in Table 1. It is clearly illustrated that the proposed scheme could save more signal energy than the reference scheme for the same α and more improvement could be obtained for greater M.

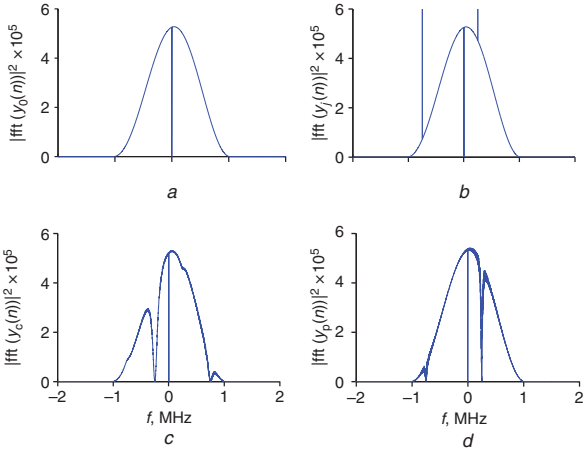

Fig. 3 *Effectivity test of anti-jamming schemes for* $\alpha = 0.99$ *and* $M = 4$

a Power spectral of clean base band signal $y_0(n)$
b Power spectral of polluted base band signal $y_j(n)$
c Power spectral of $y_c(n)$ in reference scheme
d Power spectral of $y_p(n)$ in proposed scheme

Table 1: Reserved signal power ratios for some α and M

α	$M = 2$	$M = 4$	$M = 8$
0.91	0.2152|**0.5868**	0.2158|**0.7857**	0.2149|**0.9813**
0.93	0.3125|**0.6767**	0.3129|**0.8357**	0.3120|**0.9875**
0.95	0.4539|**0.7712**	0.4537|**0.8848**	0.4531|**0.9926**
0.97	0.6454|**0.8664**	0.6446|**0.9325**	0.6443|**0.9967**
0.99	0.8775|**0.9578**	0.8766|**0.9788**	0.8766|**0.9991**

More experiments were implemented to illustrate the improvement for signal acquisition, and the peak-to-mean ratio (PMR) of the circular cross-correlation between the complex base band signal and the local base band copy with Doppler frequency $|f_d| \leq 10$ kHz is introduced for different noise-to-signal ratio ($NSR = 10\log_{10}(N_0/P_s)$) and JSRs. Especially, the jamming detection error is constrained as zero. The simulation results are shown in Fig. 4 for $\alpha = 0.99$, $M = 8$, $0 \leq NSR \leq 30$ dB and $-10 \leq JSR \leq 20$ dB. Fig. 4*a* shows the PMR for the complex base band signal polluted by noise without notch filtering. Fig. 4*b* shows the PMR for the complex base band signal polluted by noise and by jamming without notch filtering. Fig. 4*c* shows the PMR for the complex base band $y_c(n)$ in the reference scheme. Fig. 4*d* shows the PMR for the complex base band $y_p(n)$ in the proposed scheme. Experiment results show that the PMR in Figs. 4*c* and *d* approximate to the best one in Fig. 4*a*, and are obviously higher than the worst one in Fig. 4*b*. It proves that the proposed scheme and the reference scheme could improve the acquisition capability in the condition of jamming. The difference between the PMR in Figs. 4*d* and *c* is shown in Fig. 5. The PMR in Fig. 4*d* performs better than the one in Fig. 4*c* for $-10 \leq JSR \leq 17$ dB, however it is not satisfied for $JSR > 17$ dB due to strong jamming energy, which could be rejected more by the decrease α in the proposed scheme.

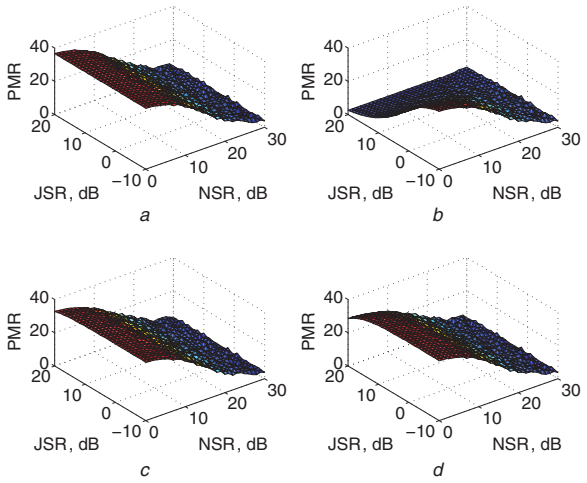

Fig. 4 *PMR test of anti-jamming schemes for* $\alpha = 0.99$ *and* $M = 8$

a PMR for $y_0(n)$ polluted only by noise
b PMR for $y_j(n)$ polluted by noise and by jamming
c PMR for $y_c(n)$ in reference scheme
d PMR for $y_p(n)$ in proposed scheme

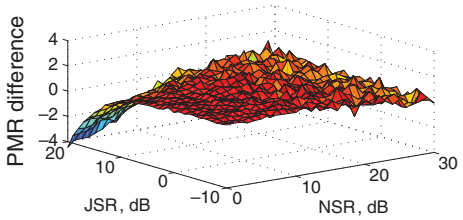

Fig. 5 *Difference between PMR in Figs. 4d and c*

Conclusion: We have developed an improved anti-jamming scheme for. The scheme has been tested by numerical simulation. Experiment results show that the proposed scheme can improve the anti-jamming capability of DSSS receivers by detecting jamming and rejecting jamming on the base band instead of the IF band.

Submitted: *25 September 2015*
doi: 10.1049/el.2015.3304
One or more of the Figures in this Letter are available in colour online.

Weihua Dai, Chunjie Qiao, Yueke Wang and Chao Zhou (*College of Mechatronics Engineering and Automation, National University of Defense Technology, Changsha 410073, People's Republic of China*)

✉ E-mail: 13755027628@163.com

References

1 Borio, D., Camoriano, L., Savasta, S., and Presti, L.L.: 'Time–frequency excision for GNSS applications', *IEEE Syst. J.*, 2008, **2**, (1), pp. 27–37
2 Savasta, S., Presti, L.L., and Rao, M.: 'Interference mitigation in GNSS receivers by a time–frequency approach', *IEEE Trans. Aerosp. Electron. Syst*, 2013, **49**, (1), pp. 415–438
3 Zhang, Y., and Amin, M.: 'Anti-jamming GPS receiver with reduced phase distortions', *IEEE Signal Process. Lett.*, 2012, **19**, (10), pp. 635–638
4 Rusch, L.A., and Poor, H.V.: 'Narrowband interference suppression in CDMA spread spectrum communications', *IEEE Trans. Commun.*, 1994, **42**, (2–4), pp. 1969–1979
5 Palestini, C., Pedone, R., Villanti, M., and Corazza, G.: 'Integrated NAV-COM systems: assisted code acquisition and interference mitigation', *IEEE Syst. J.*, 2008, **2**, (1), pp. 48–61
6 Balaei, A.T., and Dempster, A.G.: 'A statistical inference technique for GPS interference detection', *IEEE Trans. Aerosp. Electron. Syst.*, 2009, **45**, (5), pp. 1499–1509